

Molecular dynamics study of the threshold displacement energy in vanadium

L. A. Zepeda-Ruiz,* S. Han, D. J. Srolovitz, and R. Car

Princeton Materials Institute, Princeton University, Princeton, New Jersey 08544

B. D. Wirth

Chemistry and Materials Science Directorate, Lawrence Livermore National Laboratory, P.O. Box 808, L-353, Livermore, California 94550

(Received 27 September 2002; revised manuscript received 27 January 2003; published 28 April 2003)

The threshold displacement energy (TDE) is calculated for vanadium as a function of temperature and orientation by molecular dynamics simulations. The TDE varies from 13 to 51 eV, depending on orientation and is nearly temperature independent between 100 and 900 K. The lowest TDE is in the $\langle 100 \rangle$ direction. We characterize the defects associated with the displacement simulations and found that they consist of vacancies and $\langle 111 \rangle$ -split dumbbells.

DOI: 10.1103/PhysRevB.67.134114

PACS number(s): 61.80.Az, 61.72.Ji, 61.82.Bg

I. INTRODUCTION

The prediction of the long term behavior of the materials that will form the first wall of fusion power systems is particularly challenging for several reasons. First, 14-MeV neutrons produced by the deuterium-tritium fusion reaction are not readily available in sufficient quantity for systematic materials development. Second, some of the materials (e.g., vanadium alloys) are only available in limited quantities. In addition, damage production and accumulation take place over time scales as small as 10^{-13} sec (collisions) and as large as 10^9 sec (reactor lifetimes). The microstructure, composition profile, and properties of these alloys evolve continuously over these time scales.

While SiC, vanadium alloys, martensitic steels, and copper alloys are all materials of interest for the fusion program, the present study focuses on vanadium, because of its prominence in the U.S. fusion program.¹ Vanadium exhibits an excellent combination of thermal conductivity, thermal expansion, elastic modulus, heat flux capability, compatibility with lithium, radiation swelling, and ductility.

Because of the intrinsic difficulty in obtaining experimental data, a critical need exists for the prediction of the properties and evolution of V alloys under fusion reactor conditions. Several types of computer simulations of radiation damage have been exploited in recent years.^{2,3} An evolving paradigm for modeling radiation damage uses a combination of simulation techniques that allows information obtained on small time scales to be used on progressively longer time scales. Such a multiscale modeling approach typically involves molecular dynamics (MD) simulations of the initial displacement cascades for times up to a nanosecond,⁴⁻⁶ followed by kinetic Monte Carlo modeling of the evolution of the point defect distributions for times up to milliseconds,^{7,8} and statistical mechanics/continuum models for long term evolution (up to years).⁹

One of the most important physical parameters for describing radiation damage is the threshold displacement energy (TDE). The TDE is the minimum kinetic energy transferred to an atom in the lattice from an impinging particle necessary to permanently displace an atom from its lattice site, thus generating a stable defect, such as a Frenkel pair. In

the case of high kinetic energy particle impingement (such as 14-MeV neutrons in a fusion reactor environment), the initial cascade gives rise to a series of subcascades which stop when the highest energy particle has kinetic energy smaller than the TDE. Hence, threshold displacement energies are critical parameters for both low and high energy irradiation conditions. The TDE provides a lower limit on particle kinetic energies that must be considered in MD simulations of radiation damage and, hence, is a key parameter for enabling MD simulations of displacement cascades. The TDE has been determined both experimentally^{10,11} and through MD simulations¹²⁻¹⁵ for several materials. However, no work has been reported so far for vanadium.

In the present study, we employ molecular dynamics simulations to determine the threshold displacement energy for vanadium as a function of both the orientation of the incident particle momentum and temperature. The MD simulations are compared to results for other materials and also provide information on the type of point defects produced during irradiation, which gives a partial explanation of the directional anisotropy of the TDE.

II. COMPUTATIONAL METHOD

Since the threshold displacement energy is determined, in large part, by phenomena occurring on the atomic scale, the veracity of the simulation results can be no better than the description of the atomic interactions employed. In this study, we employ a new parameterization of an embedded atom method/Finnis-Sinclair-type potential for vanadium.¹⁶ The reparameterization was performed in order to ensure that the point defect properties are consistent with the predictions of a new set of first-principles calculations.¹⁷ The resultant potential has been extensively tested and successfully used in calculating point-defect properties in vanadium.¹⁶ The energy of atom i in a system described by this potential can be written in the following functional form¹⁸

$$E_i = \frac{1}{2} \sum_j V(r_{ij}) - \sqrt{\sum_j \phi(r_{ij})}, \quad (1)$$

TABLE I. Data used to fit the new vanadium potential. Elastic moduli come from the compilation by Simmons and Wang (Ref. 27); the unrelaxed vacancy formation energy and the cohesive energy are from Han *et al.* (Ref. 17).

Quantity	a (Å)	E_{coh} (eV)	C_{11} (eV/Å ³)	C_{12} (eV/Å ³)	C_{44} (eV/Å ³)	$E_V^{f,u}$ (eV)
Value	3.03	5.3	1.42	0.743	0.269	2.85

where the central-force pair potential, $V(r_{ij})$, and the atomic density, $\phi(r_{ij})$, are fitted with a series of cubic splines and given by

$$V(r) = \sum_{k=1}^6 a_k (r_k - r)^3 H(r_k - r) \quad (2)$$

and

$$\phi(r) = \sum_{k=1}^2 A_k (R_k - r)^3 H(R_k - r). \quad (3)$$

In Eqs. (2) and (3) r_k and R_k are knot points such that $r_1 > r_2 > r_3 > r_4 > r_5 > r_6$ and $R_1 > R_2$; and $H(x) = 0$ for $x < 0$ and $H(x) = 1$ for $x > 0$. Six parameters are fitted exactly (r_k and R_k are fixed) to reproduce the three cubic elastic constants, the cohesive energy, lattice parameter, and unrelaxed vacancy formation energy of vanadium, while the two remaining free parameters are chosen from the “effective” potential, $V(r_{ij}) - \phi(R_{ij})/\sqrt{\rho_0}$, at the nearest neighbor separation and the value of a_6 . The values of the fitting parameters and fitted coefficients are given in Tables I and II, respectively. Details on the fitting procedure can be found elsewhere.¹⁶ Finally, the very short range, repulsive part of the pairwise term in the potential [Eq. (1)] is modified based upon the Ziegler-Biersack-Littmark model.¹⁹

Threshold displacement energies in vanadium were calculated using the molecular dynamics simulation code MDCASK.²⁰ All simulations were carried out in a $10a_0 \times 10a_0 \times 10a_0$ body centered cubic crystals (a_0 is the lattice parameter of the cubic unit cell) with periodic boundary conditions. The MD simulations were performed in the canonical (NVT) ensemble at temperatures between 100 and 900 K. The system was thermalized at a given temperature that was controlled by applying Langevin dynamics²¹ to the two outer layers of atoms in the computational cell to dissipate the energy associated with the thermal spike introduced by the

TABLE II. Fitted coefficients for the new vanadium potential. r_k and R_k are in units of the bcc lattice parameter (a_0) while the coefficients a_k and A_k are in eV/ a_0^3 and eV²/ a_0^6 , respectively.

r_1	1.300000	a_1	-71.861297
r_2	1.220000	a_2	221.019869
r_3	1.150000	a_3	-203.133261
r_4	1.060000	a_4	118.249184
r_5	1.950000	a_5	-93.678070
r_6	1.866025	a_6	141.643266
R_1	1.300000	A_1	26.834293
R_2	1.200000	A_2	6.118468

displacement event. A primary knock-on atom (PKA) was chosen near the center of the simulation cell and assigned a velocity along a particular direction, consistent with a chosen knock-on energy. The trajectories of all of the atoms in the system were traced for 10 ps following the knock-on event. The TDE was defined as the minimum kinetic energy transferred by the PKA to a lattice atom that resulted in the formation of a stable Frenkel pair. In other words, we increased the kinetic energy of the knock-on event until at least one point defect pair remained at the end of the 10 ps simulation. The increment in energy applied in the procedure was 1 eV, consequently, the TDE is determined to an accuracy of ± 0.5 eV. It is important to note that the TDE obtained from MD simulations is likely a lower bound since longer time recombination processes are necessarily excluded. The coordinate system of the computational cell is shown in Fig. 1. The simulations were performed over a range of θ values for $\phi = 45^\circ$. This range of orientations includes the three highest symmetry directions in the crystals ($\langle 100 \rangle$, $\langle 110 \rangle$, and $\langle 111 \rangle$) as well as many in-between these.

III. RESULTS

A. Threshold displacement energies

In experiments, knock-on events will occur with all possible orientations of the incident particle momentum. However, the symmetry of the crystal is such that only a subset of orientations is unique. The full space can be spanned by limiting $0^\circ \leq \theta \leq 45^\circ$ and $0^\circ \leq \phi \leq 45^\circ$. However, since we fix $\phi = 45^\circ$, we expand the range of θ to $0^\circ \leq \theta \leq 90^\circ$ in order to include all of the high symmetry directions (i.e., $\langle 100 \rangle$, $\langle 110 \rangle$, and $\langle 111 \rangle$). In addition to obtaining data at a

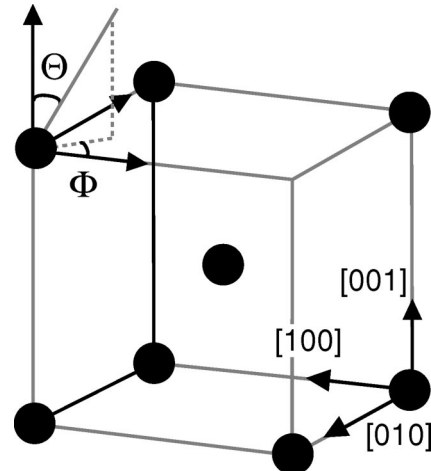


FIG. 1. Coordinate system of the computational unit cell.

TABLE III. Threshold displacement energies (TDE) for vanadium at 300 K.

Direction	θ (deg)	ϕ (deg)	TDE (eV)
[100]	0	45	13
[100] _m	2	44	15
[110]	90	45	46
[110] _m	88	44	50
[111]	54.7	45	17
[111] _m	50	44	20

uniform spacing in θ , we performed a set of calculations with the momenta of the primary knock-on atom slightly misaligned (by a few degrees) from the high symmetry orientations (denoted by the subscript m). This is done to avoid a direct (head on) collision between a V atom and its nearest neighbor along these directions.

The TDE along the three high symmetry directions (and a few degrees misaligned) at 300 K are listed in Table III. We observe that variations of a few degrees from the high symmetry directions produces only a small increase (≤ 4 eV) in the TDE compared with the differences between the three high symmetry orientations (13–50 eV). Of the three high symmetry directions, the TDE is a minimum in $\langle 100 \rangle$ and a maximum in $\langle 110 \rangle$. Figure 2 shows the variation of the threshold displacement energy with the orientation of the incident particle momentum θ , together with the experimental values obtained for Fe and Mo along the low index directions.^{22,23} To within the precision of the present measurements, the three high symmetry directions are local minima in the TDE versus θ . In addition, these are the only minima, at least for the set of orientations simulated.

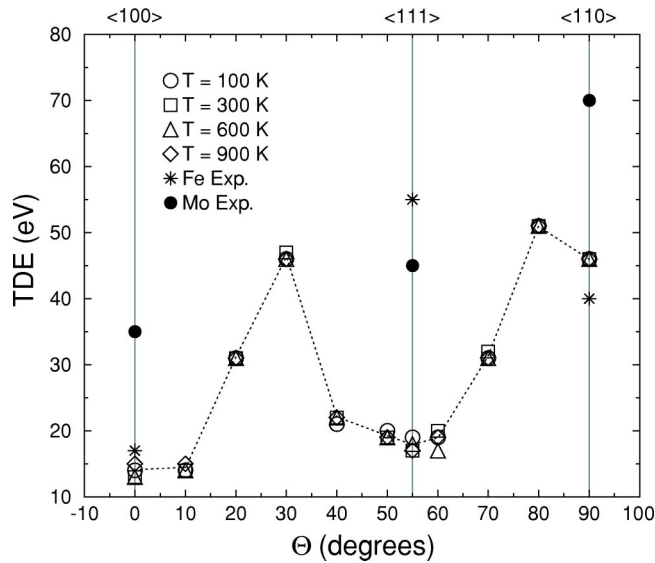


FIG. 2. Variation of the threshold displacement energy (TDE) with recoil orientation and temperature from the MD simulations (open symbols). Experimental measurements for Fe (Ref. 22) and Mo (Ref. 23) are also shown for comparison. The dashed line is a guide connecting the average of the MD results.

Figure 2 also shows the effect of temperature on the TDE for vanadium, for 100, 300, 600, and 900 K. These results show that the threshold displacement energy is independent of temperature (to within the precision of the present simulations). It is useful to consider this result in light of interstitial diffusion mechanisms in V.²⁴ The stable self-interstitial is a $\langle 111 \rangle$ -split dumbbell and migrates through a crowdion saddle point with a very low activation energy, such that interstitial diffusion occurs even at 4 K.²⁵ Thus, the observed interstitial diffusion is one-dimensional at low temperatures ($T < 700$ K) and, as a result of rotational direction changes, three-dimensional at high T .²⁴ One might expect Frenkel pair recombination to be easier at elevated temperatures. Hence, the TDE may exhibit some temperature dependence over the range of temperatures that cross the boundary between one- and three-dimensional diffusion, e.g., 600 and 900 K.

B. Defect structure

Examination of the atomic configurations following the simulations provides information on the nature of the resulting Frenkel pair, in particular, the self-interstitial atom. At the end of the 10-ps simulations, all of the self-interstitials are split dumbbells. First-principles calculations¹⁷ and atomistic simulations with the same interatomic potential as used here¹⁶ suggest that the most stable self-interstitial is a $\langle 111 \rangle$ dumbbell (i.e., a split interstitial), which is nearly degenerate with the crowdion configuration. While the previous calculations were performed at equilibrium, the present TDE simulations are far from equilibrium. Therefore, we now examine whether the $\langle 111 \rangle$ interstitial is stable under these conditions. To this end, we measured the orientation of the observed dumbbell axis with respect to the closest $\langle 111 \rangle$ direction. The results are presented in Table IV. The deviation from $\langle 111 \rangle$ ranged from 3° to 14° . These deviations are consistent with the first-principles results,¹⁷ which show that the $\langle 111 \rangle$ -dumbbell configuration is stable relative to other dumbbell orientations, but the dumbbell energy varies slowly with misorientation around the $\langle 111 \rangle$ orientation; i.e., $\partial^2 E / \partial \psi^2$ near $\langle 111 \rangle$ is small, where ψ is the deviation of the dumbbell axis from $\langle 111 \rangle$. This suggests that the angular deviations observed are either attributable to thermal fluctuations or from interactions between the self-interstitial dumbbell and the vacancy.

Following the initial transfer of momentum to a lattice atom, several atoms are displaced from their lattice sites by more than half of the nearest neighbor spacing (even at energies more than 5 eV smaller than the TDE). However, during the relaxation of the structure in the 10 ps after event initiation, many of these displaced atoms return to perfect lattice positions. While further annihilation can occur after 10 ps, this happens slowly and hence the Frenkel pair produced at the TDE is relatively stable. We observed (see Table IV) that the self-interstitial and vacancy that compose such a Frenkel pair are separated by between $2.6a_0$ and $8.1a_0$ or 8–24 Å, with typical separations close to $\sim 7a_0$ (21 Å). This suggests that self-interstitials and vacancies will annihilate if closer together than some annihilation distance which is of order 20 Å in vanadium. The few Frenkel pairs that are ob-

TABLE IV. Point-defect configurations from MD simulations of the TDE at 300 K. The split-interstitial dumbbell orientations are measured with respect to the $\langle 111 \rangle$ direction.

θ (deg)	ϕ (deg)	dumbbell orientation (deg)	distance from vacancy (a_0)
0	45	8.58	2.57
10	45	10.46	6.70
20	45	3.82	2.46
30	45	11.39	4.13
40	45	7.04	7.81
50	45	11.41	7.84
55	45	13.61	7.72
60	45	6.69	6.13
70	45	7.52	7.83
80	45	13.57	3.58
90	45	12.18	8.06

served at much shorter distances may be in the process of annihilating via vacancy diffusion or rotation of the self-interstitial dumbbells, both of which have a high activation energy compared with interstitial migration along the $\langle 111 \rangle$ direction.²⁴

IV. DISCUSSION AND CONCLUSIONS

The minimum threshold displacement energy in vanadium is approximately 13 eV. This corresponds to a displacement along the $\langle 100 \rangle$ direction. The maximum TDE observed in the simulations was 51 eV, in a direction close to $\langle 101 \rangle$. Since the simulations did not span all possible angles, it is likely that the true maximum TDE is even larger, especially when allowing for longer time recombination processes.

A comparison of the threshold displacement energy for V with experimental values for other body centered cubic metals (Fe and Mo) is shown in Fig. 2 for the low index directions.^{22,23} MD simulations for these other bcc metals generally reproduce the experimental data.^{12,13,26} The comparison shows that the directional anisotropy is comparable in Mo but the TDE ordering in $\langle 110 \rangle$ and $\langle 111 \rangle$ orientations is different in Fe. The reversal of $\langle 110 \rangle$ and $\langle 111 \rangle$ ordering is somewhat puzzling, since all three metals exhibit easy one-dimensional motion in the $\langle 111 \rangle$ crowdion direction. Even though the stable self-interstitial is a $\langle 110 \rangle$ dumbbell in both Mo and Fe. Possible explanations for the disparity of these three metals may involve the self-interstitial properties, or possibly anisotropy of the elastic constants, but this requires further investigation.

Examination of Fig. 2 demonstrates that the low index $\langle 100 \rangle$, $\langle 110 \rangle$, and $\langle 111 \rangle$ directions are orientations where the TDE is a minimum (at least for the $\phi = 45^\circ$ case considered here). The values of the TDE increases from $\langle 100 \rangle$ to $\langle 111 \rangle$ to $\langle 110 \rangle$, with the TDE for $\langle 110 \rangle$ much larger than the other two directions. The ordering of these orientations may be understood by a consideration of the local geometry through which the displaced atom must travel in order to form a Frenkel pair. An atom displaced in the $\langle 100 \rangle$ direction must traverse an orthogonal square arrangement of atoms in the $\{100\}$ plane (the atoms on the edges of the square are separated by

the bcc lattice parameter a_0). In a second case, the barrier which a $\langle 110 \rangle$ -displaced atom must cross corresponds to a rectangular arrangement of atoms (of size $a_0 \times \sqrt{2}a_0$). In both cases, the barrier is associated with the expansion of these local atom groupings within their planes. Simple geometry shows that the atomic number densities of the $\{100\}$ and $\{110\}$ planes are $1/a_0^2$ and $\sqrt{2}/a_0^2$, respectively. Since it is more difficult to expand a high density plane than a low density plane, this explains why the TDE for $\langle 100 \rangle$ is lower than that for $\langle 110 \rangle$.

An atom displaced in the close-packed $\langle 111 \rangle$ direction must traverse an equilateral triangle of atoms separated by $\sqrt{2}a_0$. The atomic number density on this plane is $1/(\sqrt{3}a_0^2)$, which is even less than that for the $\{100\}$ plane. This would suggest that the TDE for the $\langle 111 \rangle$ -displacement case should be even lower than that for the $\langle 100 \rangle$ case. This contradicts the simulation results (Fig. 2), which show that the TDE for $\langle 111 \rangle$ is slightly larger than for $\langle 100 \rangle$. This apparent discrepancy can be removed by recalling that $\langle 111 \rangle$ is the closest packed direction. Hence, the atom displaced in the $\langle 111 \rangle$ direction first directly strikes its nearest neighbor in the $\langle 111 \rangle$ direction before its center traverses the planar triangular arrangement of atoms. This initial contact raises the energy that an atom displaced along $\langle 111 \rangle$ requires one to produce a Frenkel pair over and above that expected based upon the density of atoms in the $\{111\}$ plane. As the crystallographic orientation of the atom displacement becomes a higher index, the use of the atomic plane density to predict the relative magnitudes of the TDE becomes less reliable. This can be traced to the observation that the atomic configuration that determines the barrier involves interactions between more and more neighboring atoms, thereby becoming increasingly three dimensional.

The near temperature independence of the threshold displacement energy in V is not surprising since the magnitude of the TDE is very much greater than thermal energies (even at temperatures approaching the melting point). Further, since the energy required to produce a Frenkel pair is much smaller than the TDE, a recombination of Frenkel pairs is clearly of great significance. First principles calculations suggest that the migration energies for vacancies and the

stable $\langle 111 \rangle$ -dumbbell self-interstitials are approximately 0.33 and 0.01 eV, respectively (the inherent accuracy of these calculations is ~ 0.05 eV).¹⁷ The fact that the vacancy migration energy is significantly larger than that for the self-interstitial suggests that during the initial fast recombination sequences, the vacancies are nearly immobile and it is the motion of the interstitials that is key. $\langle 111 \rangle$ -oriented self-interstitials rapidly migrate along the $\langle 111 \rangle$ directions in which they lie, but rotate into other $\langle 111 \rangle$ directions relatively slowly (with an activation energy of 0.44 eV).¹⁶ Therefore, interstitial migration is essentially one-dimensional over the time scales of the present simulations. This was confirmed by the dumbbell orientations measured in the TDE simulations performed with the interatomic potential fit to the same first-principles results.¹⁶ Therefore, if as a result of the initial displacement event the vacancy and self-interstitial dumbbells do not end up colinear (along a $\langle 111 \rangle$ direction) or nearly so, they have a low recombination probability unless their separations are very small. This gives rise to the notion of an annihilation

distance or radius, as discussed above. Unfortunately, this may be of limited utility since the actual annihilation conditions depend on the location and orientation of the dumbbell vis-à-vis the vacancy. Moreover, during longer times, vacancy migration and self-interstitial rotation may lead to additional recombination. Consequently, the present results should be viewed as a lower bound TDE.

ACKNOWLEDGMENTS

The authors gratefully acknowledge useful discussions with Graeme Ackland (University of Edinburgh) and Maria-José Caturla (Lawrence Livermore National Laboratory) and the support of the Office of Fusion Energy Sciences (Grant No. DE-FG02-01ER54628). Part of this work was performed under the auspices of the U.S. Department of Energy and Lawrence Livermore National Laboratory under Contract No. W-7405-Eng-48.

*Present address: Chemistry and Materials Science Directorate, Lawrence Livermore National Laboratory, P.O. Box 808, L-353, Livermore, California 94550.

¹H. M. Chung, B. A. Loomis, and D. L. Smith, *J. Nucl. Mater.* **239**, 139 (1996).

²F. Seitz and J. S. Koehler, *Solid State Phys.* **56**, 307 (1956).

³R. S. Averback and T. Díaz de la Rubia, *Solid State Phys.* **51**, 281 (1998).

⁴J. B. Gibson, A. N. Goland, M. Milgram, and G. H. Vineyard, *Phys. Rev.* **120**, 1229 (1960).

⁵A. J. E. Foreman, C. A. English, and W. J. Pythian, *Philos. Mag. A* **66**, 655 (1992).

⁶T. Díaz de la Rubia, *Annu. Rev. Mater. Sci.* **26**, 613 (1996).

⁷H. Heinisch and B. N. Singh, *J. Nucl. Mater.* **232**, 206 (1996).

⁸N. Soneda and T. Díaz de la Rubia, *Philos. Mag. A* **78**, 995 (1998).

⁹W. J. Pythian, R. E. Stoller, A. J. E. Foreman, A. F. Calder, and D. J. Bacon, *J. Nucl. Mater.* **233**, 2445 (1995).

¹⁰S. J. Zinkle and C. Kinoshita, *J. Nucl. Mater.* **251**, 200 (1997).

¹¹M. Biget, P. Vajda, A. Lucasson, and P. Lucasson, *Radiat. Eff.* **21**, 229 (1974).

¹²G. J. Ackland, D. J. Bacon, A. F. Calder, and T. Harry, *Philos. Mag. A* **75**, 713 (1997).

¹³R. Pasianot, M. Alurralde, A. Almazouzi, and M. Victoria, *Philos. Mag. A* **82**, 1671 (2002).

¹⁴L. Malerba and J. M. Perlado, *Phys. Rev. B* **65**, 045202 (2002).

¹⁵B. Park, W. J. Weber, and L. R. Corrales, *Phys. Rev. B* **64**, 174108 (2001).

¹⁶S. Han, L. A. Zepeda-Ruiz, G. J. Ackland, R. Car, and D. J. Srolovitz, *J. Appl. Phys.* **93**, 3328 (2003).

¹⁷S. Han, L. A. Zepeda-Ruiz, G. J. Ackland, R. Car, and D. J. Srolovitz, *Phys. Rev. B* **66**, 220101(R) (2002).

¹⁸G. J. Ackland, G. I. Tichy, V. Vitek, and M. W. Finnis, *Philos. Mag. A* **56**, 735 (1987).

¹⁹J. F. Ziegler, J. P. Biersack, and U. Littmark, *The Stopping and Range of Ions in Matter* (Pergamon, New York, 1985).

²⁰T. Díaz de la Rubia and M. W. Guinan, *J. Nucl. Mater.* **174**, 151 (1990).

²¹R. Biswas and D. R. Hamman, *Phys. Rev. B* **34**, 895 (1986).

²²P. Jung and W. Schilling, *Phys. Rev. B* **5**, 2046 (1972).

²³F. Maury, P. Vajda, M. Biget, A. Lucasson, and P. Lucasson, *Radiat. Eff.* **25**, 175 (1975).

²⁴L. A. Zepeda-Ruiz, S. Han, R. Car, D. J. Srolovitz, and G. J. Ackland (unpublished).

²⁵P. Ehrhart, P. Jung, H. Schultz, and H. Ullmaier, in *Atomic Defects in Metals*, edited by H. Ullmaier, Landolt-Börnstein, New Series, Group, III, Vol. 25 (Springer-Verlag, Berlin, 1991), p. 173.

²⁶D. J. Bacon, A. F. Calder, J. M. Harder, and S. J. Wooding, *J. Nucl. Mater.* **205**, 52 (1993).

²⁷G. Simmons and H. Wang, *Single Crystal Elastic Constants and Calculated Aggregate Properties: a Handbook* (MIT Press, Cambridge, MA, 1971).